A NEW METHOD FOR TIME–DOMAIN MODELLING OF NONLINEAR CIRCUITS IN LARGE LINEAR NETWORKS

Jean Mahseredjian Serge Lefebvre
Institut de Recherche d'Hydro–Québec (IREQ)
1800 montée Ste–Julie, Varennes
Québec, Canada J3X 1S1

Xuan–Dai Do
Ecole Polytechnique de Montréal
P. O. Box 6079, Montréal
Québec, Canada

Keywords : Modelling and simulation techniques, time–domain network analysis, nonlinear circuits, EMTP

ABSTRACT : This paper illustrates the generality of the *hybrid analysis* method for solving nonlinear circuit elements in arbitrary circuit topologies and demonstrates the theoretical ties with conventional varying topology methods for semiconductor switch representation. A new method for generating *hybrid equations* without preliminary knowledge of the topological tree is also presented. The goal is to provide more general and efficient solution methods for modelling nonlinear circuits in the EMTP (Electromagnetic Transients Program).

1. INTRODUCTION

The most common approach [1] for time–domain digital simulation of multiphase power networks is based on nodal or modified–nodal [2] analysis with fixed time–step trapezoidal integration. Discretized linear network equations are given by $\mathbf{Y_n V_n} = \mathbf{I_n}$ ($\mathbf{Y_n}$ is the nodal admittance matrix, $\mathbf{V_n}$ is the node to ground voltage vector and $\mathbf{I_n}$ is for nodal current injections) and solved directly through forward–backward substitution at each simulation time–point. The above set of equations is referred to as the main system of linear equations. The choice of nodal analysis is due to the simplicity of the equation formulation algorithm, which avoids the lengthy calculations of the topological tree. The trapezoidal integration is chosen for being a precise A–stable method which is simple to program and which requires a minimal number of history terms. The fixed time–step is mainly imposed by the presence of transmission lines, where a change of time–step would require interpolation for a large number of history terms within the propagation time delay interval. The fixed time–step also avoids costly recalculations and retriangularizations of $\mathbf{Y_n}$ in large networks, but in counterpart it has no capability for automatic error control and time–step selection according to simulated network time constants.

Large power networks are mostly linear, interconnecting a limited number of nonlinear branches. Two main methods [3] are presently available for the representation of nonlinear branch functions. In the first method a nonlinear voltage–current branch function is linearized with a Norton equivalent inserted in the main system of linear equations at each simulation time–point. It can be demonstrated that when the Norton equivalent update is non–iterative, this method is an approximate version of the solution through the Newton–Raphson algorithm [4]. The second method referenced as the *post–compensation* (also referenced as *compensation* method) algorithm, offers a simultaneous solution while applying an iterative process within only a reduced set of linear network equations. This set of equations represents the Thevenin equivalent of the linear network. Since transmission lines introduce decoupling in the Thevenin equivalent, several nonlinear branch equations can be eventually solved concurrently. This second method currently used in the EMTP [3][5], is particularly advantageous for solving nonlinearities in large linear networks, since it is simultaneous and avoids lengthy interactions with the main system of linear equations.

The *compensation* method although very powerful, is not conformable to the topological proper–tree $\mathcal{T}$ [6] and therefore has topological limitations. The *hybrid analysis* has been found [7] to be more general than the *compensation* algorithm, and can be used to model varying topologies caused by semiconductor switches in nonlinear power electronics circuits. This paper makes new contributions in addition to the approach in [7], by demonstrating how *hybrid analysis* equations can be generated and solved without preliminary knowledge of $\mathcal{T}$ and how to account for varying topological trees in a more simple algorithm than the conventional varying topology methods [8]–[11]. A new more general automatic method for extracting port equations is also presented and permits inclusion of nonlinear elements isolated by linear branches. Detailed solution steps are elaborated for topologically difficult sample circuits. This paper also contributes the extension of nonlinear branch or element representation to the concept of the multiport nonlinear circuit, which is a circuit that concentrates a large number of nonlinearities and can be advantageously solved through a minimal simultaneous connection interface with the main system of linear equations. All contributions are within the scope of an arbitrary network solution.

The presented research is justified by the steady increase of EMTP simulation needs for nonlinear elements (arc models, arresters, machines ...) in arbitrary topologies and nonlinear circuits such as power converters and flexible *ac* transmission systems.

2. CONFORMABILITY TO THE TOPOLOGICAL PROPER–TREE

The equations characterizing an $\mathcal{N}$–port [12] through the hybrid matrix $\mathbf{H}$ are given by (*hybrid equations*) :

$$\begin{bmatrix} \hat{\mathbf{i}}_v \\ \hat{\mathbf{v}}_l \end{bmatrix} = \begin{bmatrix} \mathbf{H}_{vv} & \mathbf{H}_{vl} \\ \mathbf{H}_{lv} & \mathbf{H}_{ll} \end{bmatrix} \begin{bmatrix} \hat{\mathbf{v}}_v \\ \hat{\mathbf{i}}_l \end{bmatrix} + \begin{bmatrix} \mathbf{H}_{va} & \mathbf{H}_{vb} \\ \mathbf{H}_{la} & \mathbf{H}_{lb} \end{bmatrix} \begin{bmatrix} \hat{\mathbf{v}}_a \\ \hat{\mathbf{i}}_b \end{bmatrix} \tag{1}$$

where vector $\hat{\mathbf{V}}$ is for extracted port voltages and vector $\hat{\mathbf{I}}$ stands for extracted port currents. The subscripts $\mathbf{a}$, $\mathbf{b}$, $\mathbf{v}$ and $\mathbf{l}$ are used to denote independent voltage source voltage ports, independent current source current ports, voltage ports and current ports respectively. The extracted voltage and current ports can be of any nature linear or nonlinear, but only nonlinear ports are of interest in this paper. The elements forming the $\mathcal{N}$–port are all linear and vector $\hat{\mathbf{i}}_b$ includes history terms for discrete circuit models. The nonlinear port identity (voltage or current) is not available prior to formulation of (1). The nonlinear port voltages and currents are related through the nonlinear function Φ :

$$\Phi(\hat{\mathbf{I}}_\phi, \hat{\mathbf{V}}_\phi) = \mathbf{0} \tag{2}$$

where $\hat{\mathbf{I}}_\phi = [\ \hat{\mathbf{I}}_v\ \hat{\mathbf{I}}_l\ ]^t$ and $\hat{\mathbf{V}}_\phi = [\ \hat{\mathbf{V}}_v\ \hat{\mathbf{V}}_l\ ]^t$ when ports are identified. The selection of port identity is not arbitrary. This statement can be illustrated by formulating *hybrid equations* for the circuit of Figure 1. If all nonlinear branches are modelled as current ports, then using equation (1) :

$$\hat{\mathbf{V}}_l = \mathbf{H}_{ll}\ \hat{\mathbf{I}}_l + [\ \mathbf{H}_{la}\ \mathbf{H}_{lb}\ ]\ [\ \hat{\mathbf{V}}_a\ \hat{\mathbf{I}}_b\ ]^t \tag{3}$$

in which case $\mathbf{H}_{ll} = \mathbf{0}$. This set of equations cannot be solved without adding artificial circuit elements, and is identical to :

$$\hat{\mathbf{V}}_l = \mathbf{Z}_{th}\ \hat{\mathbf{I}}_l + \mathbf{V}_{th} \tag{4}$$

with $\mathbf{Z}_{th} = \mathbf{H}_{ll}$ ($\mathbf{Z}_{th} = \mathbf{0}$ for the test case of Figure 1) and $\mathbf{V}_{th} = [\ \mathbf{H}_{la}\ \mathbf{H}_{lb}\ ][\ \hat{\mathbf{V}}_a\ \hat{\mathbf{I}}_b\ ]^t$ the Thevenin impedance and voltage respectively. This standard equation is used in the *compensation* method which can only model a nonlinear branch as a nonlinear current source.

The singular equation (3) is avoided when at least one nonlinear branch is modelled as a voltage port, to be conformable to $\mathfrak{T}$: the topological proper–tree of the circuit of Figure 1 must include at least one nonlinear voltage port in the tree branches. The *compensation* method, contrary to *hybrid analysis*, has no capability to comply with the restrictions of $\mathfrak{T}$ and is thus less general. The topological tree for the circuit of Figure 1 allows a minimum of 1 and a maximum of 3 voltage ports, the *hybrid equations* for 3 voltage ports are shown in Appendix A.

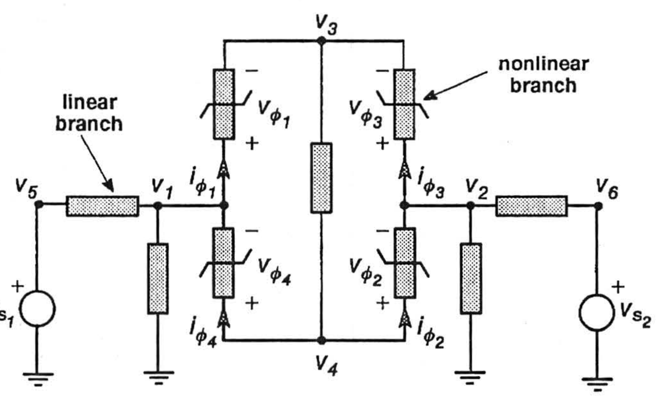

Figure 1 Test circuit

3. AUTOMATIC EXTRACTION OF HYBRID EQUATIONS

To demonstrate how equation (1) can be extracted from the nodal analysis equations in the EMTP, it is useful to recall the currently used EMTP method for calculating $\mathbf{Z}_{th}$. The basic system $\mathbf{Y}_n\,\mathbf{V}_n = \mathbf{I}_n$ is first expanded into :

$$\begin{bmatrix} \mathbf{Y}_{11} & \mathbf{Y}_{12} \\ \mathbf{Y}_{21} & \mathbf{Y}_{22} \end{bmatrix} \begin{bmatrix} \mathbf{V}_{n_1} \\ \mathbf{V}_{n_2} \end{bmatrix} = \begin{bmatrix} \mathbf{I}_{n_1} \\ \mathbf{I}_{n_2} \end{bmatrix} \tag{5}$$

and then modified to calculate $\mathbf{V}_{n_1}$ by forward backward substitution in :

$$\mathbf{U}_{11}\ \mathbf{V}_{n_1} = \mathbf{L}_{11}^{-1}\ \mathbf{I}_{n_1} - \mathbf{L}_{11}^{-1}\ \mathbf{Y}_{12}\ \mathbf{V}_{n_2} \tag{6}$$

where subscripts **1** and **2** stand for *n* unknown node voltages and *s* nodes connected to known voltage sources respectively. Matrices $\mathbf{U}_{11}$ and $\mathbf{L}_{11}$ are from the upper–lower decomposition (calculated through Gaussian elimination) of $\mathbf{Y}_{11}$. The following equations are also recalled :

$$\mathbf{V}'_{n_1} = \mathbf{V}_{n_1} + \mathbf{V}_{n\phi_1} \tag{7}$$

$$\hat{\mathbf{V}}_\phi = \mathbf{A}^t_{n\phi_1}\ \mathbf{V}'_{n_1} + \mathbf{A}^t_{n\phi_2}\ \mathbf{V}_{n_2} \tag{8}$$

$$\mathbf{U}_{11}\ \mathbf{V}_{n\phi_1} = -\ \mathbf{L}_{11}^{-1}\ \mathbf{A}_{n\phi_1}\ \hat{\mathbf{I}}_\phi \tag{9}$$

where $\mathbf{V}_{n\phi_1}$ represents the node voltage contributions from the nonlinear branch currents, $\mathbf{V}'_{n_1}$ is the vector of network node voltages after *compensation* and the node incidence matrix of *m* nonlinear branches is defined as $\mathbf{A}_{n\phi} = [\,\mathbf{A}^t_{n\phi_1}\ \mathbf{A}^t_{n\phi_2}\,]^t$ ($a_{ij} \in \mathbf{A}_{n\phi}$ and $a_{ij} = 1$ if current of branch *j* is leaving node *i*, $a_{ij} = -1$ if current of branch *j* is entering node *i* and $a_{ij} = 0$ otherwise). To calculate $\mathbf{Z}_{th}$ it is sufficient to solve equation (9) for $\mathbf{V}_{n\phi_1}$ and then to combine the resulting equation with equations (7) and (8), as follows :

$$\mathbf{V}_{n\phi_1} = \mathbf{Z}_\phi\ \hat{\mathbf{I}}_\phi \tag{10}$$

$$\mathbf{Z}_{th} = \mathbf{A}^t_{n\phi_1}\ \mathbf{Z}_\phi \tag{11}$$

$\mathbf{Z}_\phi$ is an $n \times m$ matrix. The formulation of (9) uses minimal computer memory but its solution requires *m* forward backward substitutions.

Since equation (9) makes the assumption that all nonlinear branches are modelled as nonlinear current sources, it cannot be used for generating *hybrid equations*. The following steps are applied instead. At start point, all ports besides source ports are of undetermined nature. Equation (8) is combined with equations (6), (7) and (9) to result in :

$$\begin{bmatrix} \mathbf{Y}_{11} & \mathbf{Y}_{12} & \mathbf{A}_{n\phi_1} \\ \mathbf{A}^t_{n\phi_1} & \mathbf{A}^t_{n\phi_2} & \mathbf{0} \end{bmatrix} \begin{bmatrix} \mathbf{V}'_{n_1} \\ \mathbf{V}_{n_2} \\ \hat{\mathbf{I}}_\phi \end{bmatrix} = \begin{bmatrix} \mathbf{I}_{n_1} \\ \hat{\mathbf{V}}_\phi \end{bmatrix} \tag{12}$$

with $\mathbf{V}_{n_2} = \hat{\mathbf{V}}_a$ and $\mathbf{I}_{n_1} = -\ \mathbf{A}_{nb_1}\ \hat{\mathbf{I}}_b$ (see equation (1)). The matrix $\mathbf{A}_{nb} = [\,\mathbf{A}^t_{nb_1}\ \mathbf{A}^t_{nb_2}\,]^t$ is the node incidence matrix of current source ports.

Equation (12) can be solved by applying Gaussian elimination to the upper part independently from the lower part. Although this treatment is acceptable in most of the solved cases, it is preferable to exploit the structure of (12) for solving cases where a zero pivot appears in the elimination of $\mathbf{Y}_{11}$. This is the case, for example, in Figure 1 where a linear branch (branch connected between the nodes of v_3 and v_4) is isolated from the linear network by nonlinear branches. To avoid the zero determinant matrix thus formed, it is sufficient to exchange rows with the lower part of (12) during the triangularization of $\mathbf{Y}_{11}$. When an exchange pivot is not available in $\mathbf{A}^t_{n\phi_1}$, it is feasible to create an artificial port with infinite resistance and connected to the trouble node, this is one more advantage of equation's (12) structure.

The $\mathbf{Y}_{11}$ reduction is followed by the elimination of $\mathbf{A}^t_{n\phi_1}$ for decoupling of port equations from *n* network voltages. It follows that modifications applied to equation (12) will result in :

$$\begin{bmatrix} \mathbf{U}^x & \mathbf{Y}^x_{12} & \mathbf{A}^x_{n\phi_1} \\ \mathbf{0} & \Gamma_{la} & \Pi \end{bmatrix} \begin{bmatrix} \mathbf{V}'_{n_1} \\ \hat{\mathbf{V}}_a \\ \hat{\mathbf{I}}_\phi \end{bmatrix} = \begin{bmatrix} -\ \mathbf{A}^x_{nb_1} & \mathrm{B} \\ \Gamma_{lb} & \Psi \end{bmatrix} \begin{bmatrix} \hat{\mathbf{I}}_b \\ \hat{\mathbf{V}}_\phi \end{bmatrix} \tag{13}$$

where superscript **x** indicates matrices affected by the Gaussian elimination and matrix B resulted from row exchanges. Considering the unitary elements of $\mathbf{A}^t_{n\phi_1}$ it is preferable to start by reducing it to the echelon form before elimination using upper part pivots.

Equation (13) contains two independent equations, the linear network equations :

$$\mathbf{U^x V'_{n_1}} = -\mathbf{A^x_{nb_1}} \hat{\mathbf{I}}_\mathbf{b} - \mathbf{A^x_{n\phi_1}} \hat{\mathbf{I}}_\phi - \mathbf{Y^x_{12}} \hat{\mathbf{V}}_\mathbf{a} + \mathrm{B} \hat{\mathbf{V}}_\phi \quad (14)$$

and the nonlinear port equations :

$$\Pi \hat{\mathbf{I}}_\phi = \Psi \hat{\mathbf{V}}_\phi + \Gamma [\hat{\mathbf{V}}_\mathbf{a} \hat{\mathbf{I}}_\mathbf{b}]^t \quad (15)$$

with $\Gamma = [\ -\Gamma_{la}\ \Gamma_{lb}\ ]$.

The complete extraction procedure of *hybrid equations* from equation (13), is shown in Appendix A for the circuit of Figure 1. It is based on the preliminary knowledge of port identity within the restrictions of $\mathcal{T}$. In a general case, $\mathcal{T}$ can be found by calculating the fundamental cutset matrix, but this is a lengthy and practically prohibitive process, specially for large networks. A new method for finding port identity is needed.

It must be understood that equation (15) cannot be symbolically simplified since the conditioning of matrices Π and Ψ is unknown and assuming all voltage ports or all current ports may not be in conformity with $\mathcal{T}$. The proposed solution algorithm is based on the diagonalization of matrix Π or Ψ : the choice is imposed by the needed number of voltage ports and implementation efficiency. The following demonstrations are for the limiting cases of minimal and maximal number of voltage ports.

When the requested number of voltage ports is minimal, the solution of (15) starts by the diagonalization of Ψ. By letting the ports classified in the first columns of Ψ to be more susceptible to become voltage ports, the reduction of Ψ is applied from right to left. Artificial ports with zero current, for example, are placed in the last columns of Ψ since it is preferable to keep them as current ports. At the end of the reduction process, equation (15) has the following shape :

$$\Pi' \hat{\mathbf{I}}_\phi = \Psi' \hat{\mathbf{V}}_\phi + \Gamma' [\hat{\mathbf{V}}_\mathbf{a} \hat{\mathbf{I}}_\mathbf{b}]^t \quad (16)$$

where :

$$\Psi' = [\Psi'_\mathbf{v}\ \Psi'_\mathbf{i}] \quad (17)$$

$$\Psi'_{\mathbf{v}_{ij}} = 0 \quad i = 1,\dots,m_1\ ,\ \forall j$$

$$\Psi'_{\mathbf{i}_{ij}} = 0 \quad i \neq m_1 + j\ ,\ \forall j$$

$$\Psi'_{\mathbf{i}_{ij}} = 1 \quad i = m_1 + j\ ,\ j = 1,\dots,m_2$$

$$\Pi' = [\Pi'_\mathbf{v}\ \Pi'_\mathbf{i}] \quad (18)$$

Matrices $\Psi'_\mathbf{v}$ and $\Psi'_\mathbf{i}$ are $m \times m_1$ and $m \times m_2$ respectively. The m_1 ports with null pivots in $\Psi'_\mathbf{v}$ are voltage ports. Since the diagonalization of Ψ is performed from right to left, it is clear that ports classified in the first columns of Ψ have a greater probability to remain in $\Psi'_\mathbf{v}$ during the reduction process and become voltage ports. The limiting case is $\Psi' = \Psi'_\mathbf{i}$ and $\Psi'_\mathbf{v} = \mathbf{0}$, which means that it is acceptable to have no voltage ports in $\mathcal{T}$.

To finalize the solution of (16) it is necessary to exchange $\Pi'_\mathbf{v}$ with $\Psi'_\mathbf{v}$ and to pursue with the reduction to identity of $[-\Pi'_\mathbf{v}\ \ \Psi'_\mathbf{i}]$ until $[\ \hat{\mathbf{I}}_\mathbf{v}\ \hat{\mathbf{V}}_\mathbf{i}\ ]^t$ is isolated :

$$[-\Psi'_\mathbf{v}\ \ \Pi'_\mathbf{i}] \begin{bmatrix} \hat{\mathbf{V}}_\mathbf{v} \\ \hat{\mathbf{I}}_\mathbf{i} \end{bmatrix} = [-\Pi'_\mathbf{v}\ \ \Psi'_\mathbf{i}] \begin{bmatrix} \hat{\mathbf{I}}_\mathbf{v} \\ \hat{\mathbf{V}}_\mathbf{i} \end{bmatrix} + \Gamma' \begin{bmatrix} \hat{\mathbf{V}}_\mathbf{a} \\ \hat{\mathbf{I}}_\mathbf{b} \end{bmatrix} \quad (19)$$

$$\begin{bmatrix} \hat{\mathbf{I}}_\mathbf{v} \\ \hat{\mathbf{V}}_\mathbf{i} \end{bmatrix} = [\Psi''_\mathbf{v}\ \Pi''_\mathbf{i}] \begin{bmatrix} \hat{\mathbf{V}}_\mathbf{v} \\ \hat{\mathbf{I}}_\mathbf{i} \end{bmatrix} + \Gamma'' \begin{bmatrix} \hat{\mathbf{V}}_\mathbf{a} \\ \hat{\mathbf{I}}_\mathbf{b} \end{bmatrix} \quad (20)$$

Equation (20) is equivalent to (1).

When the requested number of voltage ports is maximal, it is more efficient to start the solution of (15) by the diagonalization of Π. By letting the ports classified in the first columns of Π to be more susceptible to become voltage ports, the reduction of Π is applied from left to right, to transform equation (15) into :

$$\Pi^\square \hat{\mathbf{I}}_\phi = \Psi^\square \hat{\mathbf{V}}_\phi + \Gamma^\square [\hat{\mathbf{V}}_\mathbf{a} \hat{\mathbf{I}}_\mathbf{b}]^t \quad (21)$$

where :

$$\Pi^\square = [\Pi^\square_\mathbf{v}\ \Pi^\square_\mathbf{i}] \quad (22)$$

$$\Pi^\square_{\mathbf{v}_{ij}} = 1 \quad i = j$$

$$\Pi^\square_{\mathbf{v}_{ij}} = 0 \quad i \neq j$$

$$\Pi^\square_{\mathbf{i}_{ij}} = 0 \quad j = 1,\dots,m_2 - m_A\ ,\ i > m_1$$

$$\Psi^\square = [\Psi^\square_\mathbf{v}\ \Psi^\square_\mathbf{i}] \quad (23)$$

Matrices $\Pi^\square_\mathbf{v}$ and $\Pi^\square_\mathbf{i}$ are $m \times m_1$ and $m \times m_2$ respectively. The m_1 ports of $\Pi^\square_\mathbf{v}$ are voltage ports. The symbol m_A designates artificial current ports. The solution of (21) is finalized by exchanging $\Pi^\square_\mathbf{i}$ with $\Psi^\square_\mathbf{i}$ and isolating $[\ \hat{\mathbf{I}}_\mathbf{v}\ \hat{\mathbf{V}}_\mathbf{i}\ ]^t$ as in equation (20).

The proposed method has the ability to account for $\mathcal{T}$ without explicitly calculating it. A given circuit can have more than one $\mathcal{T}$. It follows that port identity is not unique, but can be forced through the port numbering to avoid ill–conditioned *hybrid equations*.

The calculation of *hybrid equations* for a minimal number of voltage ports and no preliminary knowledge of $\mathcal{T}$, is demonstrated for a test circuit in Appendix B.

4. VARYING TOPOLOGY REPRESENTATION

A time varying topology results when semiconductor devices such as power converter valves, are modelled as ideal switches. A switch is extracted as a nonlinear port j: $\hat{V}_{\phi_j} = 0$ ($\hat{V}_{\phi_j} \in \hat{\mathbf{V}}_\phi$) when the switch is closed and $\hat{I}_{\phi_j} = 0$ ($\hat{I}_{\phi_j} \in \hat{\mathbf{I}}_\phi$) when the switch is open. If open and closed ports are regrouped then equation (1) can be written as :

$$\begin{bmatrix} \hat{\mathbf{I}}^\ominus_\mathbf{v} \\ \hat{\mathbf{I}}^\circ_\mathbf{v} \\ \hat{\mathbf{V}}^\ominus_\mathbf{i} \\ \hat{\mathbf{V}}^\circ_\mathbf{i} \end{bmatrix} = \begin{bmatrix} \mathbf{H}^{\ominus\ominus}_\mathbf{vv} & \mathbf{H}^{\ominus\ominus}_\mathbf{vi} \\ \mathbf{H}^{\circ\ominus}_\mathbf{vv} & \mathbf{H}^{\circ\ominus}_\mathbf{vi} \\ \mathbf{H}^{\ominus\ominus}_\mathbf{iv} & \mathbf{H}^{\ominus\ominus}_\mathbf{ii} \\ \mathbf{H}^{\circ\ominus}_\mathbf{iv} & \mathbf{H}^{\circ\ominus}_\mathbf{ii} \end{bmatrix} \begin{bmatrix} \hat{\mathbf{V}}^\ominus_\mathbf{v} \\ \hat{\mathbf{I}}^\ominus_\mathbf{i} \end{bmatrix} + \begin{bmatrix} \mathbf{H}^\ominus_\mathbf{va} & \mathbf{H}^\ominus_\mathbf{vb} \\ \mathbf{H}^\circ_\mathbf{va} & \mathbf{H}^\circ_\mathbf{vb} \\ \mathbf{H}^\ominus_\mathbf{ia} & \mathbf{H}^\ominus_\mathbf{ib} \\ \mathbf{H}^\circ_\mathbf{ia} & \mathbf{H}^\circ_\mathbf{ib} \end{bmatrix} \begin{bmatrix} \hat{\mathbf{V}}_\mathbf{a} \\ \hat{\mathbf{I}}_\mathbf{b} \end{bmatrix} \quad (24)$$

where the superscript $\ominus$ stands for ports with $[\ \hat{\mathbf{V}}^\ominus_\mathbf{v}\ \hat{\mathbf{I}}^\ominus_\mathbf{i}\ ]^t \neq \mathbf{0}$ and $\circ$ stands for ports with $[\ \hat{\mathbf{V}}^\circ_\mathbf{v}\ \hat{\mathbf{I}}^\circ_\mathbf{i}\ ]^t = \mathbf{0}$. Considering that both $\hat{\mathbf{I}}^\ominus_\mathbf{v}$ and $\hat{\mathbf{V}}^\ominus_\mathbf{i}$ are related to $\hat{\mathbf{V}}^\ominus_\mathbf{v}$ and $\hat{\mathbf{I}}^\ominus_\mathbf{i}$ respectively through a piecewise linear version of Φ in equation (2), equation (24) is split in two :

$$\mathbf{M'} \begin{bmatrix} \hat{\mathbf{V}}^\ominus_\mathbf{v} \\ \hat{\mathbf{I}}^\ominus_\mathbf{i} \end{bmatrix} = \begin{bmatrix} \mathbf{H}^\ominus_\mathbf{va} & \mathbf{H}^\ominus_\mathbf{vb} \\ \mathbf{H}^\ominus_\mathbf{ia} & \mathbf{H}^\ominus_\mathbf{ib} \end{bmatrix} \begin{bmatrix} \hat{\mathbf{V}}_\mathbf{a} \\ \hat{\mathbf{I}}_\mathbf{b} \end{bmatrix} - \begin{bmatrix} \mathbf{J}^\ominus_\mathbf{v} \\ \mathbf{E}^\ominus_\mathbf{i} \end{bmatrix} \quad (25)$$

$$\begin{bmatrix} \hat{\mathbf{I}}^\circ_\mathbf{v} \\ \hat{\mathbf{V}}^\circ_\mathbf{i} \end{bmatrix} + \mathbf{M''} \begin{bmatrix} \hat{\mathbf{V}}^\ominus_\mathbf{v} \\ \hat{\mathbf{I}}^\ominus_\mathbf{i} \end{bmatrix} = \begin{bmatrix} \mathbf{H}^\circ_\mathbf{va} & \mathbf{H}^\circ_\mathbf{vb} \\ \mathbf{H}^\circ_\mathbf{ia} & \mathbf{H}^\circ_\mathbf{ib} \end{bmatrix} \begin{bmatrix} \hat{\mathbf{V}}_\mathbf{a} \\ \hat{\mathbf{I}}_\mathbf{b} \end{bmatrix} \quad (26)$$

$\mathbf{J}^\ominus_\mathbf{v}$ and $\mathbf{E}^\ominus_\mathbf{i}$ are time dependent linear segment current and voltage intercepts respectively. Equation (25) is solved first for $[\ \hat{\mathbf{V}}^\ominus_\mathbf{v}\ \hat{\mathbf{I}}^\ominus_\mathbf{i}\ ]^t$ which is substituted into (26) to calculate $[\ \hat{\mathbf{I}}^\circ_\mathbf{v}\ \hat{\mathbf{V}}^\circ_\mathbf{i}\ ]^t$. The size and conditioning of $\mathbf{M'}$ depend on the solved circuit topology. The size of $\mathbf{M'}$ is minimal when all closed ports are voltage ports and all open ports are current ports. If in addition all nonlinear ports are switches then $\mathbf{M}'$ and $\mathbf{M}''$ are both zero and the solution of (26) is obtained directly.

It is possible to reformulate the switch configuration in $\mathcal{T}$ at each change of switch state, in order to transfer the largest possible number of closed switch ports in the branches of $\mathcal{T}$. This is achieved by stopping the matrix Ψ (equation (16)) reduction process before its first closed port columns. The Ψ matrix elements are unitary which makes it easier to reduce. The reformulation strategy must be programmed efficiently to avoid lengthy recalculations at each change of circuit topology. The reformulation can be avoided if the initial topology *hybrid equations* have acceptable conditioning for all circuit operating modes, but then the size of $\mathbf{M}'$ is not always minimized.

Reformulation examples for the test circuit of Figure B.1 are presented in Appendix C.

5. THE THEORETICAL TIES WITH CONVENTIONAL VARYING TOPOLOGY METHODS

The purpose of this section is to provide a practical demonstration to the fact that conventional varying topology methods [8]–[11] are enlisted in the more simple concept of *hybrid analysis.* The shown varying topology equations are for the general case where ordinary linear branches can also be part of the links of $\mathcal{T}$ in addition to valves (modelled as ideal switches), contrary to more limited presentations such as in [9]–[11].

If vector $\tilde{\mathbf{I}}_\mathbf{b}$ stands for branch currents of $\mathcal{T}$ and $\tilde{\mathbf{I}}_\ell$ for link currents of $\mathcal{T}$, then $\tilde{\mathbf{I}}_\mathbf{b} = -\tilde{\mathbf{D}}_\mathbf{c}\tilde{\mathbf{I}}_\ell$ where $\tilde{\mathbf{D}} = [\mathbf{1}\ \tilde{\mathbf{D}}_\mathbf{c}]$ is the fundamental cutset matrix [6]. The matrix $\tilde{\mathbf{D}}$ is also used to relate tree link and branch voltages : $\tilde{\mathbf{V}}_\ell = \tilde{\mathbf{D}}_\mathbf{c}^t\,\tilde{\mathbf{V}}_\mathbf{b}$. When branches are regrouped according to their type :

$$\begin{bmatrix}\tilde{\mathbf{I}}_{\mathbf{b}_o}\\ \tilde{\mathbf{I}}_{\mathbf{b}_\upsilon}\end{bmatrix} = -\begin{bmatrix}\tilde{\mathbf{D}}_{\mathbf{c}_{oo}} & \tilde{\mathbf{D}}_{\mathbf{c}_{o\upsilon}}\\ \tilde{\mathbf{D}}_{\mathbf{c}_{\upsilon o}} & \tilde{\mathbf{D}}_{\mathbf{c}_{\upsilon\upsilon}}\end{bmatrix}\begin{bmatrix}\tilde{\mathbf{I}}_{\ell_o}\\ \tilde{\mathbf{I}}_{\ell_\upsilon}\end{bmatrix} \tag{27}$$

$$\begin{bmatrix}\tilde{\mathbf{V}}_{\ell_o}\\ \tilde{\mathbf{V}}_{\ell_\upsilon}\end{bmatrix} = \begin{bmatrix}\tilde{\mathbf{D}}^t_{\mathbf{c}_{oo}} & \tilde{\mathbf{D}}^t_{\mathbf{c}_{o\upsilon}}\\ \tilde{\mathbf{D}}^t_{\mathbf{c}_{\upsilon o}} & \tilde{\mathbf{D}}^t_{\mathbf{c}_{\upsilon\upsilon}}\end{bmatrix}\begin{bmatrix}\tilde{\mathbf{V}}_{\mathbf{b}_o}\\ \tilde{\mathbf{V}}_{\mathbf{b}_\upsilon}\end{bmatrix} \tag{28}$$

where the subscripts o and υ are used to distinguish linear and nonlinear (switches) branches. The tree branches are characterized by :

$$\tilde{\mathbf{V}}_\mathbf{b} = \tilde{\mathbf{Z}}_\mathbf{b}\,\tilde{\mathbf{I}}_\mathbf{b} + \tilde{\mathbf{E}}_\mathbf{b} \tag{29}$$

This equation is general and in the most simple cases $\tilde{\mathbf{Z}}_\mathbf{b}$ is a diagonal matrix (no coupling between branches) composed of $\tilde{\mathbf{Z}}_{\mathbf{b}_{oo}}$ and $\tilde{\mathbf{Z}}_{\mathbf{b}_{\upsilon\upsilon}}$. In this presentation the coefficients of $\tilde{\mathbf{Z}}_\mathbf{b}$ are discretized equivalents and vector $\tilde{\mathbf{E}}_\mathbf{b}$ includes history terms in addition to independent voltage sources. When equations (27) and (28) are combined with (29), the following set of equations follows :

$$\begin{bmatrix}\tilde{\mathbf{V}}_{\ell_o}\\ \tilde{\mathbf{V}}_{\ell_\upsilon}\end{bmatrix} = \begin{bmatrix}\tilde{\mathbf{D}}^t_{\mathbf{c}_{oo}} & \tilde{\mathbf{D}}^t_{\mathbf{c}_{o\upsilon}}\\ \tilde{\mathbf{D}}^t_{\mathbf{c}_{\upsilon o}} & \tilde{\mathbf{D}}^t_{\mathbf{c}_{\upsilon\upsilon}}\end{bmatrix}\begin{bmatrix}\tilde{\mathbf{E}}_{\mathbf{b}_o}\\ \tilde{\mathbf{E}}_{\mathbf{b}_\upsilon}\end{bmatrix} - \tag{30}$$

$$\begin{bmatrix}\tilde{\mathbf{D}}^t_{\mathbf{c}_{oo}}\tilde{\mathbf{Z}}_{\mathbf{b}_{oo}}\tilde{\mathbf{D}}_{\mathbf{c}_{oo}} + \tilde{\mathbf{D}}^t_{\mathbf{c}_{o\upsilon}}\tilde{\mathbf{Z}}_{\mathbf{b}_{\upsilon\upsilon}}\tilde{\mathbf{D}}_{\mathbf{c}_{\upsilon o}} & \tilde{\mathbf{D}}^t_{\mathbf{c}_{oo}}\tilde{\mathbf{Z}}_{\mathbf{b}_{oo}}\tilde{\mathbf{D}}_{\mathbf{c}_{o\upsilon}} + \tilde{\mathbf{D}}^t_{\mathbf{c}_{o\upsilon}}\tilde{\mathbf{Z}}_{\mathbf{b}_{\upsilon\upsilon}}\tilde{\mathbf{D}}_{\mathbf{c}_{\upsilon\upsilon}}\\ \tilde{\mathbf{D}}^t_{\mathbf{c}_{\upsilon o}}\tilde{\mathbf{Z}}_{\mathbf{b}_{oo}}\tilde{\mathbf{D}}_{\mathbf{c}_{oo}} + \tilde{\mathbf{D}}^t_{\mathbf{c}_{\upsilon\upsilon}}\tilde{\mathbf{Z}}_{\mathbf{b}_{\upsilon\upsilon}}\tilde{\mathbf{D}}_{\mathbf{c}_{\upsilon o}} & \tilde{\mathbf{D}}^t_{\mathbf{c}_{\upsilon o}}\tilde{\mathbf{Z}}_{\mathbf{b}_{oo}}\tilde{\mathbf{D}}_{\mathbf{c}_{o\upsilon}} + \tilde{\mathbf{D}}^t_{\mathbf{c}_{\upsilon o}}\tilde{\mathbf{Z}}_{\mathbf{b}_{\upsilon\upsilon}}\tilde{\mathbf{D}}_{\mathbf{c}_{\upsilon\upsilon}}\end{bmatrix}\begin{bmatrix}\tilde{\mathbf{I}}_{\ell_o}\\ \tilde{\mathbf{I}}_{\ell_\upsilon}\end{bmatrix}$$

This equation can be solved knowing that $\tilde{\mathbf{Z}}_{\mathbf{b}_{\upsilon\upsilon}} = \mathbf{0}$ (the switches in the tree branches are closed), $\tilde{I}_{\ell_{\upsilon_j}} = 0$ ($\tilde{I}_{\ell_{\upsilon_j}} \in \tilde{\mathbf{I}}_{\ell_\upsilon}$) if switch j is open and $\tilde{V}_{\ell_{\upsilon_j}} = 0$ if switch j is closed. The linear tree links are described by :

$$\tilde{\mathbf{F}}_{\ell_{oo}}\tilde{\mathbf{V}}_{\ell_o} + \tilde{\mathbf{Z}}_{\ell_{oo}}\tilde{\mathbf{I}}_{\ell_o} + \tilde{\mathbf{E}}_{\ell_o} = \mathbf{0} \tag{31}$$

where $\tilde{\mathbf{E}}_{\ell_o}$ is the vector of history terms and independent current sources and $\tilde{\mathbf{F}}_{\ell_{oo}} = -[\mathbf{1}\ \mathbf{0}]^t$ when current sources are set to occupy the last cells in the link list.

Equation (30) must be reformulated when a switch in the branches of $\mathcal{T}$ goes into its off state ($\tilde{Z}_{\mathbf{b}_{\upsilon\upsilon_{jj}}} = \infty$). The reformulation algorithm is based on diakoptics [8]. When one or more conducting valves change their state, the currents of $\tilde{\mathbf{I}}_{\ell_\upsilon}$ are no more independent; $\tilde{\mathbf{I}}_\ell$ is now related to its reduced version $\tilde{\mathbf{I}}'_\ell$ through the transformation matrix $\tilde{\mathbf{C}}_\mathbf{T}$:

$$\begin{bmatrix}\tilde{\mathbf{I}}_{\ell_o}\\ \tilde{\mathbf{I}}_{\ell_\upsilon}\end{bmatrix} = \tilde{\mathbf{C}}_\mathbf{T}\begin{bmatrix}\tilde{\mathbf{I}}_{\ell_o}\\ \tilde{\mathbf{I}}'_{\ell_\upsilon}\end{bmatrix} \tag{32}$$

Equation (32) is replaced into (30), both sides of which are multiplied by $\tilde{\mathbf{C}}_\mathbf{T}^t$. The basic reformulation principle is simple but the automatic synthesis of $\tilde{\mathbf{C}}_\mathbf{T}$ from $\tilde{\mathbf{D}}_\mathbf{c}$ is complicated [8], specially with more than one switch in the tree branches.

A judicious combination of equations (27)–(29) and (31) can isolate vectors $\tilde{\mathbf{I}}_{\mathbf{b}_\upsilon}$, $\tilde{\mathbf{I}}_{\ell_\upsilon}$, $\tilde{\mathbf{V}}_{\mathbf{b}_\upsilon}$ and $\tilde{\mathbf{V}}_{\ell_\upsilon}$, but to avoid explicit matrix inversions it is preferable to apply *tableau analysis* by juxtaposing equations (27)–(29) and (31) :

$$\begin{bmatrix}\mathbf{1} & \mathbf{0} & \tilde{\mathbf{D}}_{\mathbf{c}_{oo}} & \mathbf{0} & \mathbf{0} & \tilde{\mathbf{D}}_{\mathbf{c}_{o\upsilon}} & \mathbf{0} & \mathbf{0}\\ \mathbf{0} & \mathbf{1} & \mathbf{0} & -\tilde{\mathbf{D}}^t_{\mathbf{c}_{oo}} & \mathbf{0} & \mathbf{0} & -\tilde{\mathbf{D}}^t_{\mathbf{c}_{o\upsilon}} & \mathbf{0}\\ \mathbf{0} & \mathbf{0} & \tilde{\mathbf{D}}_{\mathbf{c}_{\upsilon o}} & \mathbf{0} & \mathbf{1} & \tilde{\mathbf{D}}_{\mathbf{c}_{\upsilon\upsilon}} & \mathbf{0} & \mathbf{0}\\ \mathbf{0} & \mathbf{0} & \mathbf{0} & -\tilde{\mathbf{D}}^t_{\mathbf{c}_{\upsilon o}} & \mathbf{0} & \mathbf{0} & -\tilde{\mathbf{D}}^t_{\mathbf{c}_{\upsilon\upsilon}} & \mathbf{1}\\ \tilde{\mathbf{Z}}_{\mathbf{b}_{oo}} & \mathbf{0} & \mathbf{0} & -\mathbf{1} & \mathbf{0} & \mathbf{0} & \mathbf{0} & \mathbf{0}\\ \mathbf{0} & \tilde{\mathbf{F}}_{\ell_{oo}} & \tilde{\mathbf{Z}}_{\ell_{oo}} & \mathbf{0} & \mathbf{0} & \mathbf{0} & \mathbf{0} & \mathbf{0}\end{bmatrix}\begin{bmatrix}\tilde{\mathbf{I}}_{\mathbf{b}_o}\\ \tilde{\mathbf{V}}_{\ell_o}\\ \tilde{\mathbf{I}}_{\ell_o}\\ \tilde{\mathbf{V}}_{\mathbf{b}_o}\\ \tilde{\mathbf{I}}_{\mathbf{b}_\upsilon}\\ \tilde{\mathbf{I}}_{\ell_\upsilon}\\ \tilde{\mathbf{V}}_{\mathbf{b}_\upsilon}\\ \tilde{\mathbf{V}}_{\ell_\upsilon}\end{bmatrix} = \begin{bmatrix}\mathbf{0}\\ \mathbf{0}\\ \mathbf{0}\\ \mathbf{0}\\ -\tilde{\mathbf{E}}_{\mathbf{b}_o}\\ -\tilde{\mathbf{E}}_{\ell_o}\end{bmatrix} \tag{33}$$

When Gaussian elimination is applied to eliminate the framed part of the left side matrix, the following set of equations becomes decoupled :

$$\tilde{\Pi}\begin{bmatrix}\tilde{\mathbf{I}}_{\mathbf{b}_\upsilon}\\ \tilde{\mathbf{I}}_{\ell_\upsilon}\end{bmatrix} + \tilde{\Psi}\begin{bmatrix}\tilde{\mathbf{V}}_{\mathbf{b}_\upsilon}\\ \tilde{\mathbf{V}}_{\ell_\upsilon}\end{bmatrix} = \tilde{\Gamma}\begin{bmatrix}\tilde{\mathbf{E}}_{\mathbf{b}_o}\\ \tilde{\mathbf{E}}_{\ell_o}\end{bmatrix} \tag{34}$$

This is identical to equation (15) when ports are identified, observing that : $\tilde{\Pi} \doteq \Pi$, $\tilde{\Psi} \doteq -\Psi$, $\tilde{\Gamma} \doteq \Gamma$, $\tilde{\mathbf{E}}_{\mathbf{b}_o} \doteq \hat{\mathbf{V}}_\mathbf{a}$, $\tilde{\mathbf{E}}_{\ell_o} \doteq \hat{\mathbf{I}}_\mathbf{b}$, $\tilde{\mathbf{I}}_{\mathbf{b}_\upsilon} \doteq \hat{\mathbf{I}}_\mathbf{v}$, $\tilde{\mathbf{I}}_{\ell_\upsilon} \doteq \hat{\mathbf{I}}_\mathbf{l}$, $\tilde{\mathbf{V}}_{\mathbf{b}_\upsilon} \doteq \hat{\mathbf{V}}_\mathbf{v}$ and $\tilde{\mathbf{V}}_{\ell_\upsilon} \doteq \hat{\mathbf{V}}_\mathbf{l}$. It follows that the traditional equations used to describe a varying topology are closely linked to the much more simple concept of *hybrid analysis.* In fact the passage from (33) to (34) constitutes another (much less efficient) method [12] for automatic extraction of (15). The advantage of *hybrid equations* is that the unknowns are only nonlinear port variables, they can be easily extracted from and implemented into simple nodal analysis equations and their reformulation process at topological changes does not require the knowledge of $\tilde{\mathbf{D}}$ and lengthy manipulations with the transformation matrix $\tilde{\mathbf{C}}_{\mathbf{T}}$.

In equation (30) all switches in the tree branches must be in their on state to avoid ill–conditioning. Which means that for some circuits (such as Figure 1 when all nonlinear branches are not conducting) or operating modes, conformability to $\mathcal{T}$ cannot be achieved. This is not the case with the varying topology representation through *hybrid equations*, where a switch in its open state can be included in the branches of $\mathcal{T}$.

6. THE NONLINEAR CIRCUIT CONCEPT

The formulation of (12) is more efficient and general than (9). It extracts nonlinear port equations that can use voltage or current ports in arbitrary topologies and uses a single step for finding $\mathbf{V}'_{\mathbf{n}_1}$ (equation (14)). In contrast, the formulation of (9) can only represent current ports, nonlinear branches connected to voltage sources are unacceptable and $\mathbf{V}'_{\mathbf{n}_1}$ is found from (7) which combines the two additional calculation steps for $\mathbf{V}_{\mathbf{n}_1}$ from (6) and $\mathbf{V}_{\mathbf{n}\phi_1}$ from (10).

The structure of (12) becomes identical to modified nodal analysis when the s voltage source nodes are transferred into the list of n unknown node voltages :

$$\begin{bmatrix} \mathbf{Y_n} & \mathbf{A_{ns}} & \mathbf{A_{n\phi}} \\ \mathbf{A^t_{ns}} & \mathbf{0} & \mathbf{0} \\ \mathbf{A^t_{n\phi}} & \mathbf{0} & \mathbf{0} \end{bmatrix} \begin{bmatrix} \mathbf{V}'_{\mathbf{n}_1} \\ \hat{\mathbf{I}}_{\mathbf{s}} \\ \hat{\mathbf{I}}_{\phi} \end{bmatrix} = \begin{bmatrix} \mathbf{I}_{\mathbf{n}_1} \\ \hat{\mathbf{V}}_{\mathbf{s}} \\ \hat{\mathbf{V}}_{\phi} \end{bmatrix} \tag{35}$$

where $\mathbf{A_{ns}}$ is the node incidence matrix of voltage sources. The left hand side matrix of this equation is now completely symmetric and the nonlinear port equations are extracted the same way (as from (12)). The Gaussian elimination of (35) with row interchanges, can be efficiently implemented [2].

The formulation efficiency of (12) and the following method for generating port equations, should not be compared with equations (9) to (11), since, as explained in Section 2, these equations are restrictive and do not apply to arbitrary interconnections of nonlinear branches. The performance of equations (12) and (35) can be however criticized for its memory requirements and fill–in for a large number of nonlinear branches within large linear networks. The computational effort is then reduced by isolating (when possible) several nonlinear branches in a nonlinear circuit. This isolation is achieved through a limited number of port variables seen in the main linear circuit. The nonlinear circuit is simply a multiport nonlinear branch that assembles and solves its own set of linear equations and *hybrid equations*. A set (more than one) of nonlinear branches located in the same subnetwork (coupled through *hybrid equations*) has also been designated as a nonlinear circuit in this paper.

Isolation is naturally provided by specialized network equipments such as power converters, static compensators or other sophisticated multiport circuits. The pre–specified establishment of the nonlinear circuit borders is intended to limit the number of interconnections with the surrounding linear circuit, while concentrating the largest possible number of nonlinearities.

7. NUMERICAL EXAMPLE

The proposed new method (NM) is numerically verified for the nonlinear circuit of Figure 2. It is a simple high–voltage six–pulse power converter circuit. The surrounding network is assembled in the EMTP (including filters) and shown in its discretized Thevenin equivalent form. The surrounding network sees the nonlinear circuit as 4 (3 *ac* side and 1 *dc* side) nonlinear current ports. The short–circuit ratio of the *ac* network is $\approx$**6** . The current control is provided through the EMTP TACS module. The transformer and other not shown data can be found in [7]. The valves are modelled as ideal switches. This test case includes *ac* filters composed of the paralleled branches $R_{\mathcal{F}_1} - L_{\mathcal{F}_1} - C_{\mathcal{F}_1}$ and $R_{\mathcal{F}_1} - L_{\mathcal{F}_1} - C_{\mathcal{F}_2}$ where $R_{\mathcal{F}_1} = 10\Omega$, $L_{\mathcal{F}_1} = 1.104\text{H}$, $C_{\mathcal{F}_1} = .255\mu\text{F}$ and $C_{\mathcal{F}_2} = .130\mu\text{F}$.

After assembling equation (12) for this now reduced circuit, equations (14) and (15) are automatically generated. The *hybrid equations* are calculated according to the converter operating modes and the reformulation method. The following methods must be considered :

1□ no reformulation, unless necessary;

2□ a maximum number of conducting valves is transferred into tree branches;

3□ same as 2□ but storage of matrices $\mathbf{M}'$ and $\mathbf{M}''$ for repetitive operating modes.

In method 1□ when *hybrid equations* are calculated for a maximum number of voltage ports (valves 1 to 4 are voltage ports) then conditioning of $\mathbf{M}'$ remains acceptable for almost all converter modes. Reformulation may still be necessary for some extremely abnormal modes. If for example, the valves 1 to 4 are conducting and valves 5 and/or 6 are fired, then $\mathbf{M}'$ is ill–conditioned and it is necessary to transfer the conducting current ports (valves 5 and/or 6) into the branches of $\mathcal{T}$. The maximum size of $\mathbf{M}'$ is 9x9, considering that the transformer current–flux characteristic is nonlinear.

In method 2□ the *hybrid equations* are recalculated at each topological change. Although this method has an overall slower performance, since it requires frequent reformulations of the *hybrid equations*, it is more general than 1□ because there is no presumption on the performance with the maximum or minimum number of voltage ports. This method is also in accordance with the varying topology method reformulation strategy. The purpose of method 3□ is merely to improve the performance of 2□ over 1□ specially in long simulation cases. Although the efficiency of 3□ is closely linked to the actual programming of memorized matrix extraction and rearrangements, it has been noticed that for the test case of Figure 2, when only standard repetitive operating modes are encountered, method 3□ has a $\approx$40% performance increase compared to 1□. This number will decrease to $\approx$10% when matrices $\mathbf{M}'$ and $\mathbf{M}''$ are also memorized for method 1□ . Further research is needed to be able to prescribe one method or the other for a general circuit : it is a matter of tradeoff between the sizes of $\mathbf{M}'$ and $\mathbf{M}''$ and the time required to bring in new matrices at every commutation of a given circuit.

The simulation results are presented in Figures 3 and 4 and compared with the standard EMTP method, where the complete simulated network is assembled as usual. This comparison has been made possible by enabling EMTP to model valves as ideal switches with no artificial numerical snubbers in parallel. The snubbers were necessary to eliminate numerical oscillations caused by current discontinuities. The discontinuities are now suppressed using halved time–step Euler backward integration [13] within the trapezoidal method. This is a new option (not available in the current EMTP version V2 [5]) that has been recently [14] implemented in a developer's version for future release to the general EMTP users.

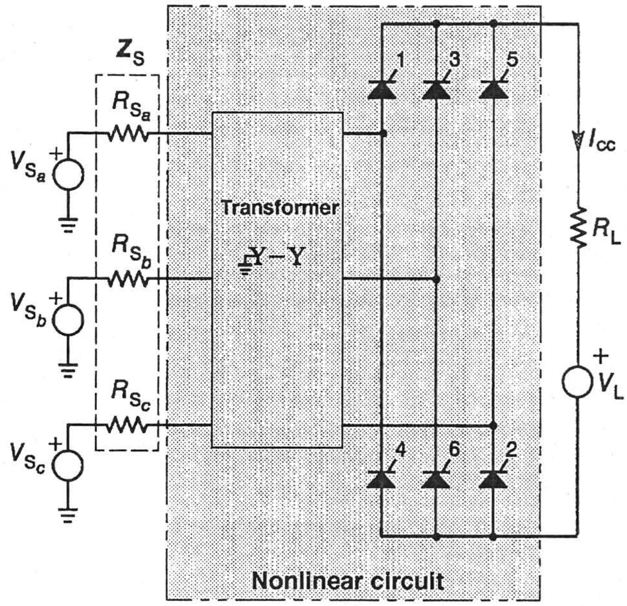

Figure 2 The tested nonlinear circuit

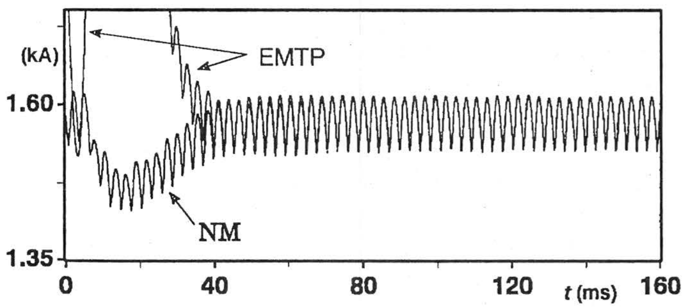

Figure 3 Current I_{cc} (see Figure 2)

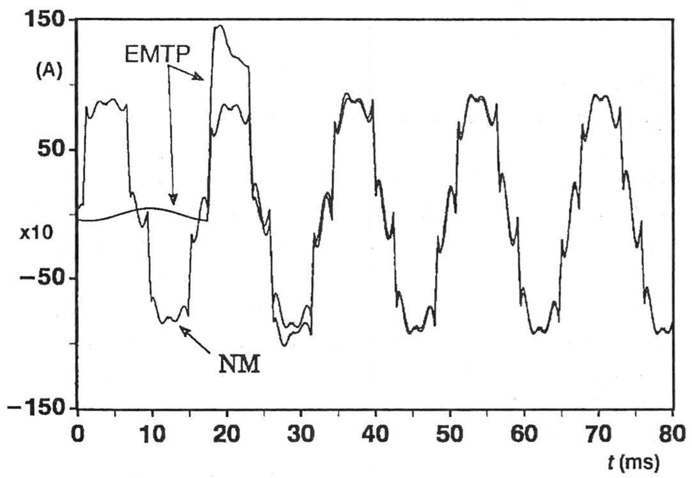

Figure 4 Converter phase a current before filters

The objective of Figures 3 and 4 is to validate method NM for modelling valves as ideal switches and all the corresponding automatic solution algorithms.The fast initialization presented and discussed in [7], is achieved through the interface with the main system of linear equations, by predicting history terms at simulation startup and iterating to find the most likely valve conduction states. This capability is one more advantage that cab be exploited in the nonlinear circuit concept. In the EMTP the initially conducting valves are predicted manually and there is no initialization algorithm. The performance ratio of the NM over the EMTP (it is estimated that NM is 3 times faster than EMTP for the shown test case) increases with the size of the surrounding network. At each change of valve state the EMTP requires complete retriangularization of its large $\mathbf{Y_n}$, contrary to the NM which reformulates only a reduced set of *hybrid equations*. It must be recalled that the generality of *hybrid equations* in the NM also allows usage of nonlinear equations for valve models.

CONCLUSIONS

This paper applied *hybrid analysis* for solving nonlinear circuits in the EMTP. It demonstrated how to extract *hybrid equations* from nodal or modified nodal analysis without preliminary knowledge of the topological proper–tree. The *hybrid equations* have also been applied to simulate varying topology networks. The simple concept of *hybrid analysis* has been theoretically linked to sophisticated conventional varying topology methods.

A typical nonlinear circuit has been solved and compared with the EMTP results.

APPENDIX A
THE HYBRID EQUATIONS FOR THE CIRCUIT OF FIGURE 1

When $\hat{\mathbf{V}}_\mathbf{v} = [\, v_{\phi_1}\ v_{\phi_2}\ v_{\phi_3}\,]^t$ (3 voltage ports) and $\hat{\mathbf{I}}_\mathbf{I} = i_{\phi_4}$ then equation (1) results in :

$$\begin{bmatrix} i_{\phi_1} \\ i_{\phi_2} \\ i_{\phi_3} \\ v_{\phi_4} \end{bmatrix} = \begin{bmatrix} \mathbf{H_{vv}} & \mathbf{H_{vI}} \\ \mathbf{H_{Iv}} & \mathbf{H_{II}} \end{bmatrix} \begin{bmatrix} v_{\phi_1} \\ v_{\phi_2} \\ v_{\phi_3} \\ i_{\phi_4} \end{bmatrix} + \begin{bmatrix} \mathbf{H_{va}} \\ \mathbf{H_{Ia}} \end{bmatrix} \begin{bmatrix} v_{s_1} \\ v_{s_2} \end{bmatrix} \tag{A.1}$$

If the linear branches connected to the nodes of v_1 and v_2 are 10 Ω resistances and the linear branch between the nodes of v_3 and v_4 is a 5 Ω resistance, then :

$$\left[\begin{array}{cccc|cc|cccc} .2 & 0 & 0 & 0 & -.1 & 0 & 1 & 0 & 0 & -1 \\ 0 & .2 & 0 & 0 & 0 & -.1 & 0 & -1 & 1 & 0 \\ 0 & 0 & .2 & -.2 & 0 & 0 & -1 & 0 & -1 & 0 \\ 0 & 0 & -.2 & .2 & 0 & 0 & 0 & 1 & 0 & 1 \\ \hline 1 & 0 & -1 & 0 & 0 & 0 & 0 & 0 & 0 & 0 \\ 0 & -1 & 0 & 1 & 0 & 0 & 0 & 0 & 0 & 0 \\ 0 & 1 & -1 & 0 & 0 & 0 & 0 & 0 & 0 & 0 \\ -1 & 0 & 0 & 1 & 0 & 0 & 0 & 0 & 0 & 0 \end{array}\right] \begin{bmatrix} v_1 \\ v_2 \\ v_3 \\ v_4 \\ v_5 \\ v_6 \\ i_{\phi_1} \\ i_{\phi_2} \\ i_{\phi_3} \\ i_{\phi_4} \end{bmatrix} = \left[\begin{array}{c} 0 \\ 0 \\ 0 \\ 0 \\ \hline v_{\phi_1} \\ v_{\phi_2} \\ v_{\phi_3} \\ v_{\phi_4} \end{array}\right] \tag{A.2}$$

Gaussian elimination stops at the 4th column. The final result is :

$$\left[\begin{array}{cccc|cc|cccc} 1 & 0 & 0 & 0 & -.5 & 0 & 5 & 0 & 0 & -5 \\ 0 & 1 & 0 & 0 & 0 & -.5 & 0 & -5 & 5 & 0 \\ 0 & 0 & 1 & -1 & 0 & 0 & -5 & 0 & -5 & 0 \\ 0 & 0 & 0 & 1 & -.5 & 0 & 5 & 0 & 0 & -5 \\ \hline 0 & 0 & 0 & 0 & 0 & 0 & -5 & 0 & -5 & 0 \\ 0 & 0 & 0 & 0 & .5 & -.5 & -5 & -5 & 5 & 5 \\ 0 & 0 & 0 & 0 & 0 & 0 & -5 & 0 & -5 & 0 \\ 0 & 0 & 0 & 0 & 0 & 0 & 0 & 5 & 0 & 5 \end{array}\right] \begin{bmatrix} v_1 \\ v_2 \\ v_3 \\ v_4 \\ v_5 \\ v_6 \\ i_{\phi_1} \\ i_{\phi_2} \\ i_{\phi_3} \\ i_{\phi_4} \end{bmatrix} = \left[\begin{array}{cccc} 0 & 0 & 0 & 0 \\ 0 & 0 & 0 & 0 \\ 0 & 0 & 0 & 0 \\ 0 & 0 & 0 & 1 \\ \hline 1 & 0 & 0 & 1 \\ 0 & 1 & 0 & -1 \\ 0 & 1 & 1 & 0 \\ 0 & -1 & -1 & 0 \end{array}\right] \begin{bmatrix} v_{\phi_1} \\ v_{\phi_2} \\ v_{\phi_3} \\ v_{\phi_4} \end{bmatrix} \tag{A.3}$$

where rows 4 and 8 have been exchanged to avoid the singularity of the linear network matrix. Nonlinear port equations are now decoupled from the linear network equations and after rearranging, according to port identity, they are given by :

$$\begin{bmatrix} i_{\phi_1} \\ i_{\phi_2} \\ i_{\phi_3} \\ v_{\phi_4} \end{bmatrix} = \begin{bmatrix} -.1 & 0 & .1 & 1 \\ 0 & -.2 & -.2 & -1 \\ .1 & -.2 & -.3 & -1 \\ -1 & 1 & 1 & 0 \end{bmatrix} \begin{bmatrix} v_{\phi_1} \\ v_{\phi_2} \\ v_{\phi_3} \\ i_{\phi_4} \end{bmatrix} + \begin{bmatrix} .05 & -.05 \\ 0 & 0 \\ -.05 & .05 \\ 0 & 0 \end{bmatrix} \begin{bmatrix} v_5 \\ v_6 \end{bmatrix} \tag{A.4}$$

with $v_5 = v_{s_1}$ and $v_6 = v_{s_2}$

APPENDIX B
TEST CIRCUIT FOR FINDING PORT IDENTITY

The studied circuit is shown in Figure B.1, it is a simplified (for demonstration purposes) version of a six–pulse power converter. The port variables are $\hat{\mathbf{I}}_\phi = [\,\hat{I}_1\ \hat{I}_2\ \hat{I}_3\ \hat{I}_4\ \hat{I}_5\ \hat{I}_6\ \hat{I}_7\,]^t$, $\hat{\mathbf{V}}_\phi = [\,\hat{V}_1\ \hat{V}_2\ \hat{V}_3\ \hat{V}_4\ \hat{V}_5\ \hat{V}_6\ \hat{V}_7\,]^t$ and $\hat{\mathbf{V}}_a = [\,V_a\ V_b\ V_c\,]^t$. The ports 1 to 6 are for valves 1 to 6 respectively. The *7th* port is an artificial port ($\hat{I}_7 = 0$) connected from the V_d^- node to ground and used to avoid singularity for the linear equations. This artificial port is added for demonstration purposes only, since other exchange pivots are available. The circuit data is : $Z_{eq} = 0.1\Omega$ and $R_L = 10\Omega$.

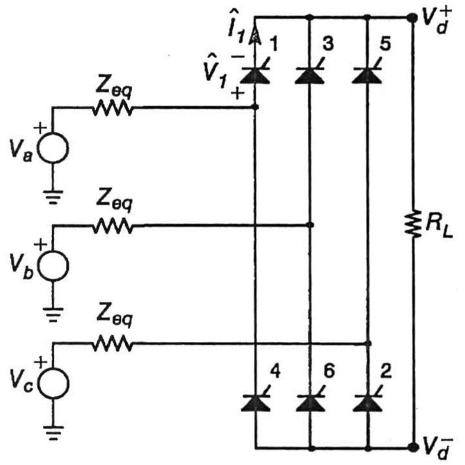

Figure B.1 Simplified six–pulse power converter circuit

Equation (15) is found to be :

$$\underbrace{\begin{bmatrix} -10.1 & 0 & -10 & .1 & -10 & 0 & 0 \\ -10 & 0 & -10 & 0 & -10 & 0 & 0 \\ -10 & 0 & -10.1 & 0 & -10 & .1 & 0 \\ -10 & 0 & -10 & 0 & -10 & 0 & 0 \\ -10 & .1 & -10 & 0 & -10.1 & 0 & 0 \\ -10 & 0 & -10 & 0 & -10 & 0 & 0 \\ -1 & 1 & -1 & 1 & -1 & 1 & 1 \end{bmatrix}}_{\Pi} \hat{\mathbf{I}}_\phi =$$

$$\underbrace{\begin{bmatrix} 1 & 0 & 0 & 0 & 0 & 0 & 1 \\ 0 & 1 & 0 & 0 & 1 & 0 & 0 \\ 0 & 0 & 1 & 0 & 0 & 0 & 1 \\ 1 & 0 & 0 & 1 & 0 & 0 & 0 \\ 0 & 0 & 0 & 0 & 1 & 0 & 1 \\ 0 & 0 & 1 & 0 & 0 & 1 & 0 \\ 0 & 0 & 0 & 0 & 0 & 0 & 0 \end{bmatrix}}_{\Psi} \hat{\mathbf{V}}_\phi + \underbrace{\begin{bmatrix} -1 & 0 & 0 \\ 0 & 0 & 0 \\ 0 & -1 & 0 \\ 0 & 0 & 0 \\ 0 & 0 & -1 \\ 0 & 0 & 0 \\ 0 & 0 & 0 \end{bmatrix}}_{\Gamma} \begin{bmatrix} V_a \\ V_b \\ V_c \end{bmatrix} \tag{B.1}$$

The reduction to identity of matrix Ψ is applied to find a minimal number of voltage ports :

$$\underbrace{\begin{bmatrix} -1 & 1 & -1 & 1 & -1 & 1 & 1 \\ -10.1 & -.1 & -10 & .1 & -9.9 & 0 & 0 \\ .1 & 0 & -.1 & -.1 & 0 & .1 & 0 \\ -10 & 0 & -10 & 0 & -10 & 0 & 0 \\ .1 & .1 & 0 & -.1 & -.1 & 0 & 0 \\ -10.1 & 0 & -9.9 & .1 & -10 & -.1 & 0 \\ -10.1 & 0 & -10 & .1 & -10 & 0 & 0 \end{bmatrix}}_{\Pi'} \hat{\mathbf{I}}_\phi =$$

$$\underbrace{\begin{bmatrix} 0 & 0 & 0 & 0 & 0 & 0 & 0 \\ 1 & 1 & 0 & 0 & 0 & 0 & 0 \\ -1 & 0 & 1 & 0 & 0 & 0 & 0 \\ 1 & 0 & 0 & 1 & 0 & 0 & 0 \\ -1 & 0 & 0 & 0 & 1 & 0 & 0 \\ 1 & 0 & 0 & 0 & 0 & 1 & 0 \\ 1 & 0 & 0 & 0 & 0 & 0 & 1 \end{bmatrix}}_{\Psi'} \hat{\mathbf{V}}_\phi + \underbrace{\begin{bmatrix} 0 & 0 & 0 \\ -1 & 0 & 1 \\ 1 & -1 & 0 \\ 0 & 0 & 0 \\ 1 & 0 & -1 \\ -1 & 1 & 0 \\ -1 & 0 & 0 \end{bmatrix}}_{\Gamma'} \begin{bmatrix} V_a \\ V_b \\ V_c \end{bmatrix} \tag{B.2}$$

The null pivot appearing in the first column of Ψ' indicates that valve 1 is a voltage port, which is in agreement with the proper–tree of this circuit. The *hybrid equations* are found after exchanging columns of $\hat{I}_1$ and $\hat{V}_1$ and isolating $[\,\hat{\mathbf{I}}_v\ \hat{\mathbf{V}}_I\,]^t$:

$$\begin{bmatrix} \hat{I}_1 \\ \hat{V}_2 \\ \hat{V}_3 \\ \hat{V}_4 \\ \hat{V}_5 \\ \hat{V}_6 \end{bmatrix} = \begin{bmatrix} 0 & 1 & -1 & 1 & -1 & 1 \\ -1 & -10.2 & .1 & -10 & .2 & -10.1 \\ 1 & .1 & -.2 & 0 & -.1 & .2 \\ -1 & -10 & 0 & -10 & 0 & -10 \\ 1 & .2 & -.1 & 0 & -.2 & .1 \\ -1 & -10.1 & .2 & -10 & .1 & -10.2 \end{bmatrix} \begin{bmatrix} \hat{V}_1 \\ \hat{I}_2 \\ \hat{I}_3 \\ \hat{I}_4 \\ \hat{I}_5 \\ \hat{I}_6 \end{bmatrix} + \begin{bmatrix} 0 & 0 & 0 \\ 1 & 0 & -1 \\ -1 & 1 & 0 \\ 0 & 0 & 0 \\ -1 & 0 & 1 \\ 1 & -1 & 0 \end{bmatrix} \begin{bmatrix} V_a \\ V_b \\ V_c \end{bmatrix} \tag{B.3}$$

Since $\hat{I}_7 = 0$ for the artificial port, the equation for $\hat{V}_7$ is supplementary.

APPENDIX C
EXAMPLES OF VARYING TOPOLOGY REPRESENTATION

In the test circuit of Figure B.1 all valves are modelled as ideal switches. If only the valves 1 and 2 are conducting and modelled as voltage ports, then the following equation is found from equation (B.2) :

$$\begin{bmatrix} \hat{I}_1 \\ \hat{I}_2 \\ \hat{V}_3 \\ \hat{V}_4 \\ \hat{V}_5 \\ \hat{V}_6 \end{bmatrix} = \begin{bmatrix} .0980 & 0 & -.0980 \\ .0980 & 0 & -.0980 \\ -.9902 & 1 & -.0098 \\ -.9804 & 0 & .9804 \\ -.9804 & 0 & .9804 \\ .0098 & -1 & .9902 \end{bmatrix} \begin{bmatrix} V_a \\ V_b \\ V_c \end{bmatrix} \tag{C.1}$$

In this case matrices $\mathbf{M}'$ and $\mathbf{M}''$ are both zero.

If valves 1, 2 and 3 are conducting and only valve 1 is modelled as a voltage port, then equations (25) and (26) are found from (B.3) :

$$\underbrace{\begin{bmatrix} 10.2 & -.1 \\ -.1 & .2 \end{bmatrix}}_{\mathbf{M}'}\begin{bmatrix} \hat{I}_2 \\ \hat{I}_3 \end{bmatrix} = \begin{bmatrix} .1 & 0 & -1 \\ -1 & 1 & 0 \end{bmatrix}\begin{bmatrix} V_a \\ V_b \\ V_c \end{bmatrix} \quad (C.2)$$

$$\begin{bmatrix} \hat{I}_1 \\ \hat{V}_4 \\ \hat{V}_5 \\ \hat{V}_6 \end{bmatrix} + \underbrace{\begin{bmatrix} -1 & 1 \\ 10 & 0 \\ -.2 & .1 \\ 10.1 & -.2 \end{bmatrix}}_{\mathbf{M}''}\begin{bmatrix} \hat{I}_2 \\ \hat{I}_3 \end{bmatrix} = \begin{bmatrix} 0 & 0 & 0 \\ 0 & 0 & 0 \\ -1 & 0 & 1 \\ 1 & -1 & 0 \end{bmatrix}\begin{bmatrix} V_a \\ V_b \\ V_c \end{bmatrix} \quad (C.3)$$

Since valves 1, 2 and 3 can belong to the proper–tree branches, it is feasible in this case to find *hybrid equations* where **M′** and **M″** are both zero. It must be concluded that the reformulation strategy depends on the previous operating mode and the efficiency of the reformulation programming.

REFERENCES

[1] H. W. Dommel : Digital computer solution of electromagnetic transients in single and multiphase networks. IEEE Trans. PAS–88, pp. 388–398, 1969

[2] L. W. Nagel : SPICE2 A computer program to simulate semiconductor circuits. Memorandum No. UCB/ERL M520, 9 May 1975

[3] H. W. Dommel : Nonlinear and time–varying elements in digital simulation of electromagnetic transients. IEEE Trans. PAS, vol. 90, pp. 2561–2567, 1971

[4] L. O. Chua and N. N. Wang : A new approach to overcome the overflow problem in computer–aided analysis of nonlinear resistive circuits. International Journal of circuit theory and applications. vol. 3, pp. 261–282, 1975

[5] Electric Power Research Institute, EMTP Development Coordination Group, EPRI EL–6421–L : Electromagnetic Transients Program Rule Book, Version 2

[6] V. Rajagopalan, M. N. S. Swamy and K. S. Rao : Formulation of state equations for R–L–C networks with modified proper trees. Proc. IEEE, Aug. 1976, pp. 1247–1248

[7] J. Mahseredjian, S. Lefebvre and D. Mukhedkar : Power Converter simulation module connected to the EMTP. IEEE Trans. on Power Systems, vol. 6, no. 2, pp. 501–510, May 1991

[8] C. M. Ong, C. T. Liu and C. N. Lu : Generation of connection matrices for digital simulation of converter circuits using the tensor approach. IEEE Trans. vol. PWRS–2, No. 4, 1987, pp. 906–912

[9] R. H. Kitchin : New method for digital–computer evaluation of converter harmonics in power systems using state variable analysis. IEE Proc., vol. 128, no. 4, pp. 196–208, July 1981

[10] K. R. Padiyar and Sachchidanand : Digital simulation of multiterminal HVDC systems using a novel converter model. IEEE Trans. PAS, vol. 102, no. 6, pp. 1624–1632, June 1983

[11] J. L. Hay and N. G. Hingorani : Dynamic simulation of multi–converter HVDC systems by digital computer, Part I, Mathematical model. IEEE Trans. vol. PAS–89, pp. 218–222, feb. 1970

[12] H. C. So : On the hybrid description of a linear n–port resulting from the extraction of arbitrarily specified elements. IEEE Trans. on Circuit Theory, vol. 12, pp. 381–387, 1965

[13] J. R. Marti and J. Lin : Suppression of numerical oscillations in the EMTP. IEEE Trans. on Power Systems, vol. 4, no. 2, May 1989, pp. 739–747

[14] J. Lin : Implementation of the CDA procedure in the EMTP for suppression of numerical oscillations. IREQ Report, Hydro–Québec, March 1992